

DFT studies of dimethylaminophenyl-substituted phthalocyanine and of its silver complexes

Martin Breza

Department of Physical Chemistry, Slovak Technical University, Radlinskeho 9, SK-81237 Bratislava, Slovakia

Supplementary information

Figure S1. UV-vis spectra of neutral dmaphPcAg (full line) and dmaphPcH₂ (dashed line) in CHCl₃.

Figure S2. Time dependence of absorption spectra during photolysis of [dmaphPcAg]⁰ under LED@385 nm irradiation.

Figure S3. DFT optimized structure of ²[dmaphPcH]⁰ in CHCl₃.

Figure S4. DFT optimized structure of ²[dmaphPc]⁻ in CHCl₃.

Figure S5. DFT calculated spin density of ⁴[dmaphPcAg]⁰ in CHCl₃.

Figure S6. DFT calculated spin density of ³[dmaphPcAg]⁻ in CHCl₃.

Figure S7. DFT calculated spin density of ⁴[dmaphPcAg]²⁻ in CHCl₃.

Figure S8. DFT calculated spin density of ²[dmaphPcH]⁰ in CHCl₃

Figure S9. DFT calculated spin density of ²[dmaphPc]⁻ in CHCl₃

Figure S10. TD-DFT calculated electron transitions in ¹[dmaphPcAg]⁺ in CHCl₃.

Figure S11. TD-DFT calculated electron transitions in ³[dmaphPcAg]⁺ in CHCl₃.

Figure S12. TD-DFT calculated electron transitions in ²[dmaphPcAg]⁰ in CHCl₃.

Figure S13. TD-DFT calculated electron transitions in ⁴[dmaphPcAg]⁰ in CHCl₃.

Figure S14. TD-DFT calculated electron transitions in ¹[dmaphPcAg]⁻ in CHCl₃.

Figure S15. TD-DFT calculated electron transitions in ³[dmaphPcAg]⁻ in CHCl₃.

Figure S16. TD-DFT calculated electron transitions in ²[dmaphPcAg]²⁻ in CHCl₃.

Figure S17. TD-DFT calculated electron transitions in ⁴[dmaphPcAg]²⁻ in CHCl₃.

Figure S18. TD-DFT calculated electron transitions in ¹[dmaphPcH₂]⁰ in CHCl₃.

Figure S19. TD-DFT calculated electron transitions in ¹[dmaphPcH]⁻ in CHCl₃.

Figure S20. TD-DFT calculated electron transitions in ²[dmaphPcH]⁰ in CHCl₃.

Figure S21. TD-DFT calculated electron transitions in ¹[dmaphPc]²⁻ in CHCl₃.

Figure S22. TD-DFT calculated electron transitions in ²[dmaphPc]⁻ in CHCl₃.

References

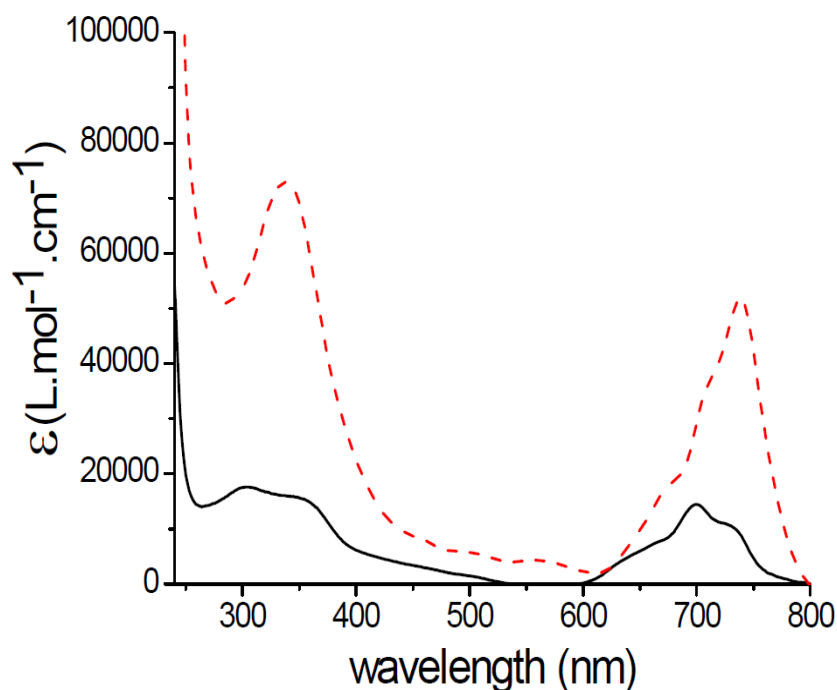


Figure S1. UV-vis spectra of neutral dmaphPcAg (full line) and dmaphPcH₂ (dashed line) in CHCl₃. Reproduced from Ref. [1] with permission from the Royal Society of Chemistry.

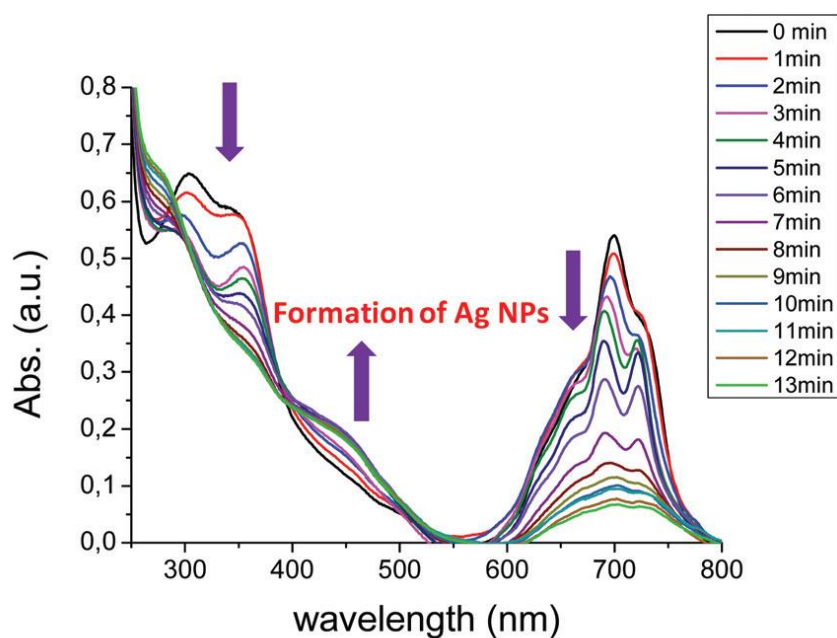


Figure S2. Time dependence of absorption spectra during photolysis of [dmaphPcAg]⁰ under LED@385 nm irradiation. LED@385 nm intensity = 470 mW cm⁻². Concentration of [dmaphPcAg]⁰ = 3.8 × 10⁻⁵ M. Solvent = CHCl₃. Reproduced from Ref. [1] with permission from the Royal Society of Chemistry.

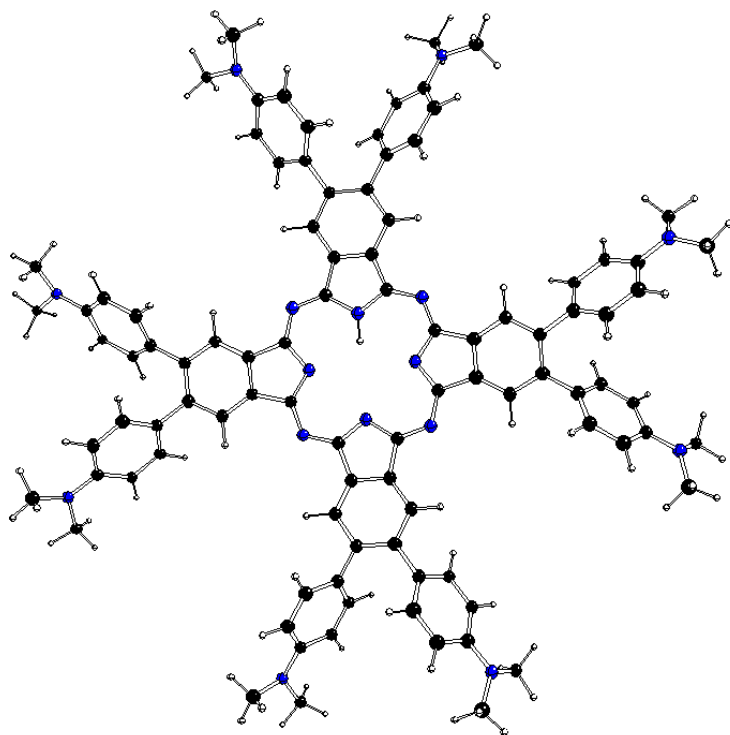


Figure S3. DFT optimized structure of $2[\text{dmaphPcH}]^0$ in CHCl_3 (C – black, N – blue, H – white).

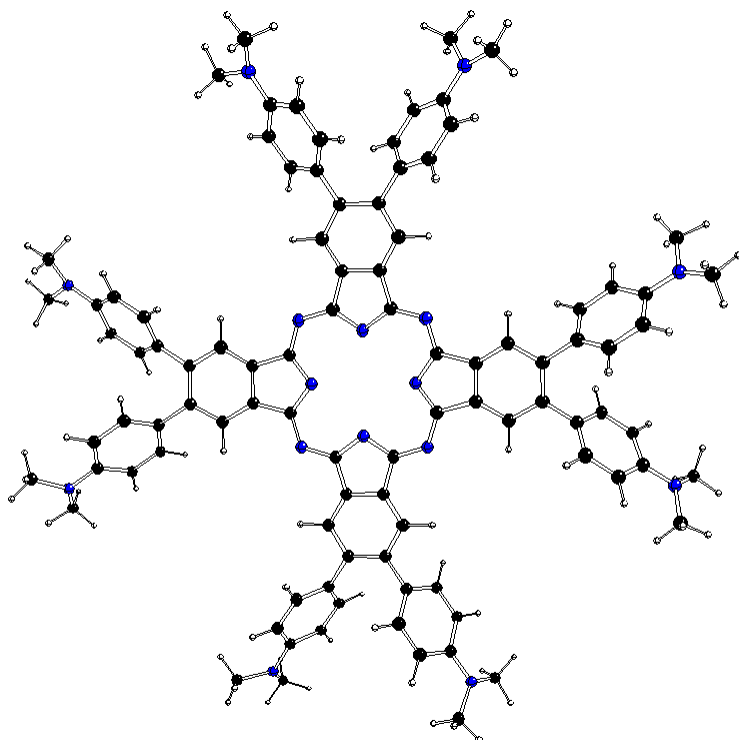


Figure S4. DFT optimized structure of $2[\text{dmaphPc}]^-$ in CHCl_3 (C – black, N – blue, H – white).

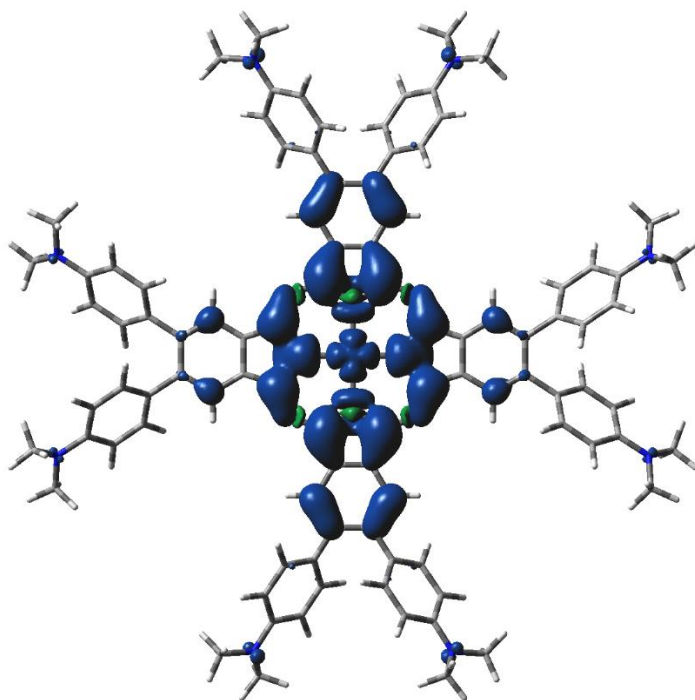


Figure S5. DFT calculated spin density of $^4[\text{dmaphPcAg}]^0$ in CHCl_3 (0.001 a.u. isosurface).

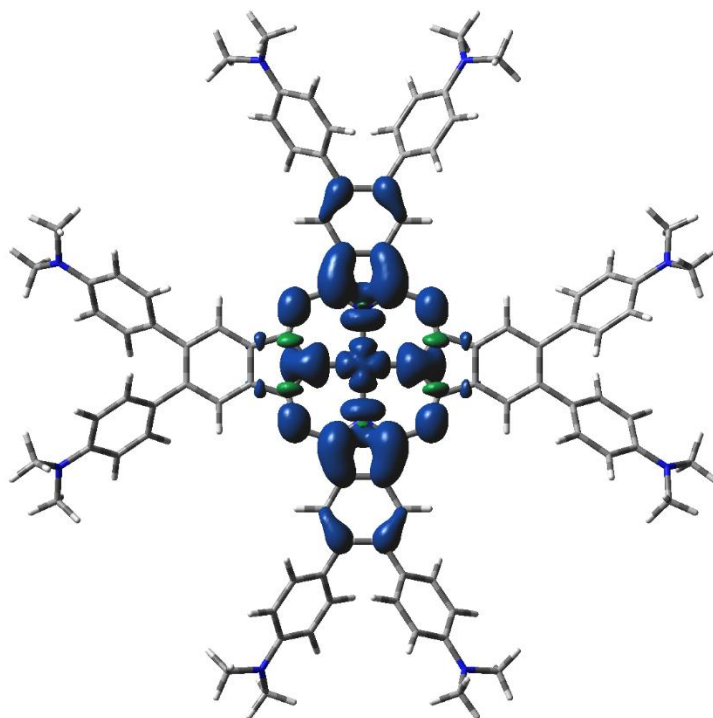


Figure S6. DFT calculated spin density of $^3[\text{dmaphPcAg}]^-$ in CHCl_3 (0.001 a.u. isosurface).

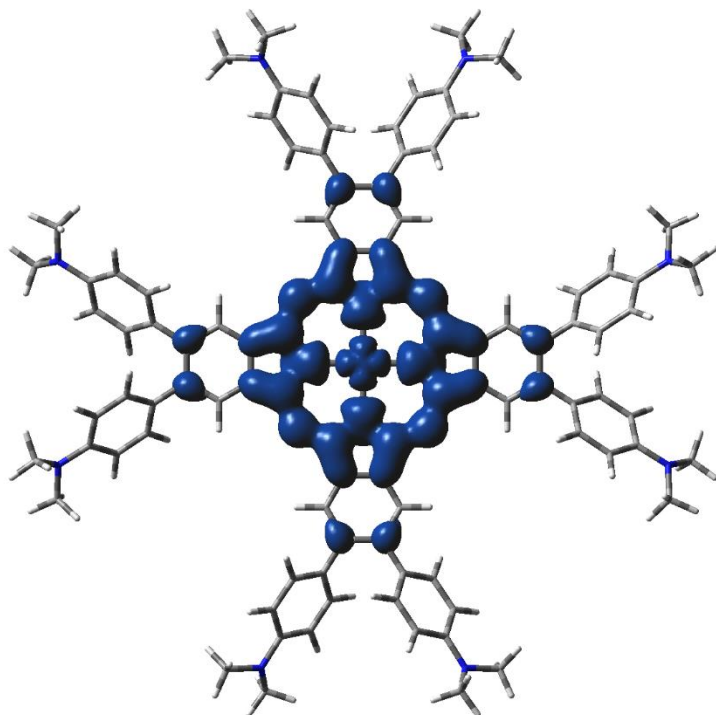


Figure S7. DFT calculated spin density of $^4[\text{dmaphPcAg}]^{2-}$ in CHCl_3 (0.001 a.u. isosurface).

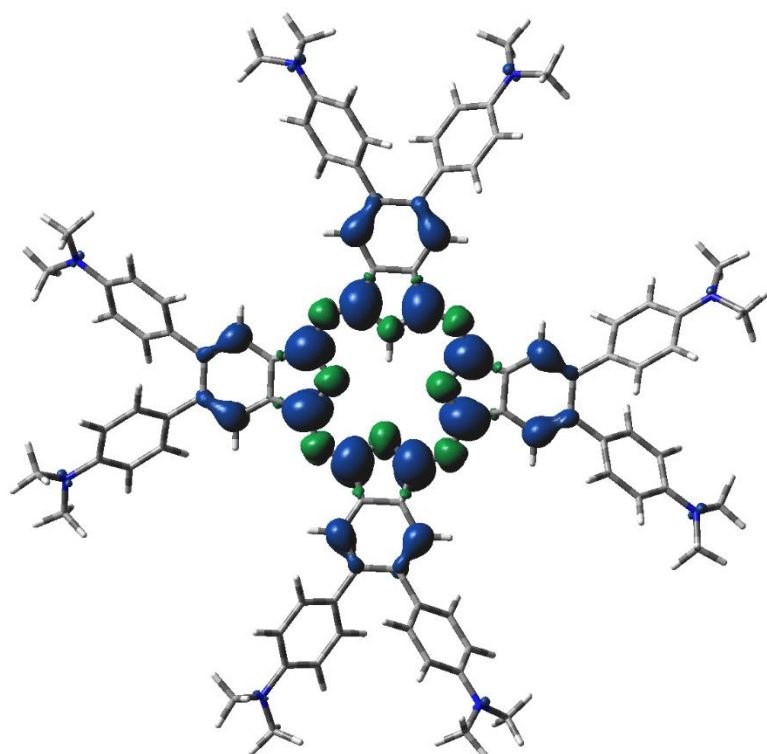


Figure S8. DFT calculated spin density of $^2[\text{dmaphPcH}]^0$ in CHCl_3 (0.001 a.u. isosurface).

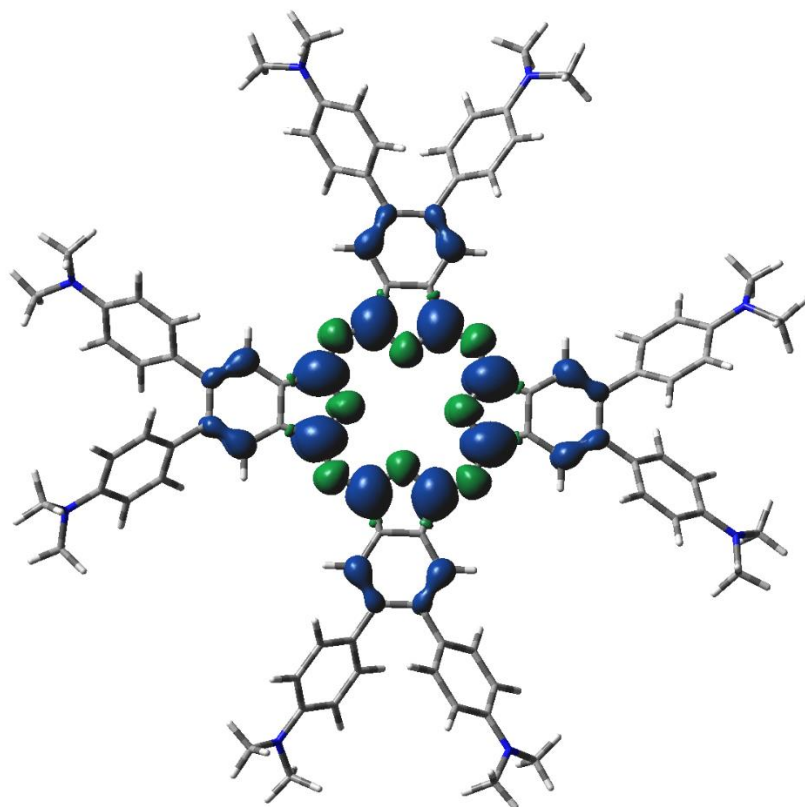


Figure S9. DFT calculated spin density of $^2[\text{dmaphPc}]^-$ in CHCl_3 (0.001 a.u. isosurface).

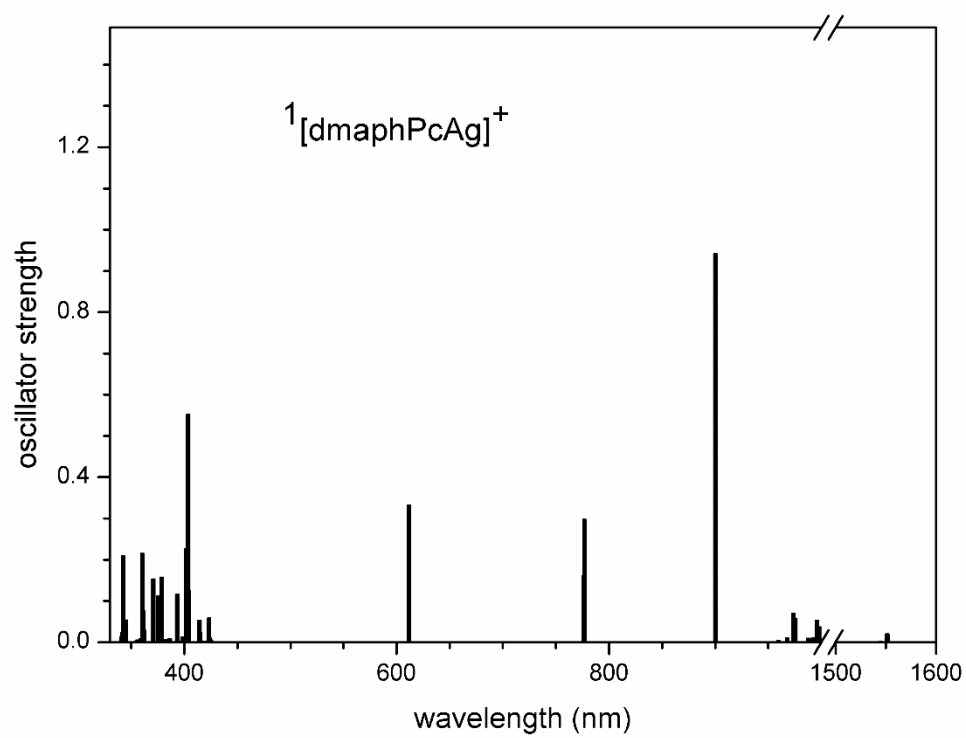


Figure S10. TD-DFT calculated electron transitions in $^1[\text{dmaphPcAg}]^+$ in CHCl_3 .

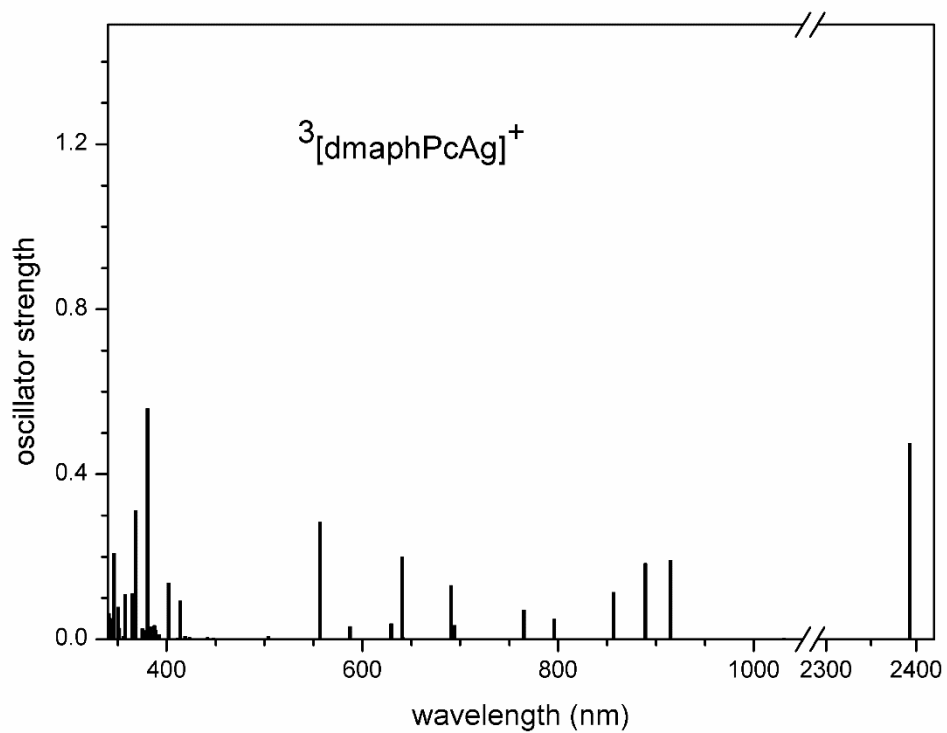


Figure S11. TD-DFT calculated electron transitions in ³[dmaphPcAg]⁺ in CHCl₃.

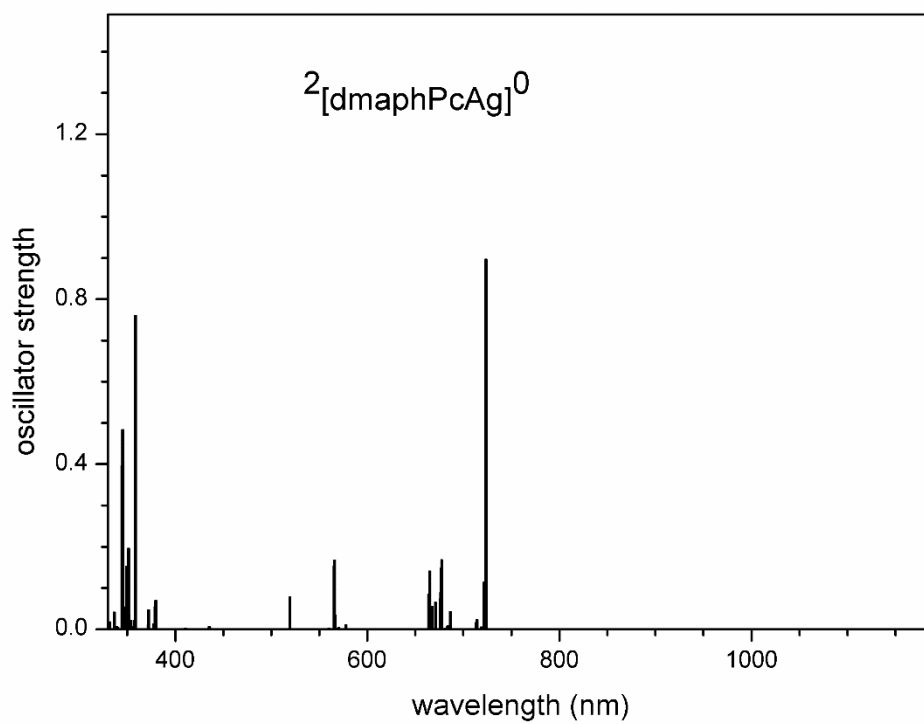


Figure S12. TD-DFT calculated electron transitions in ²[dmaphPcAg]⁰ in CHCl₃.

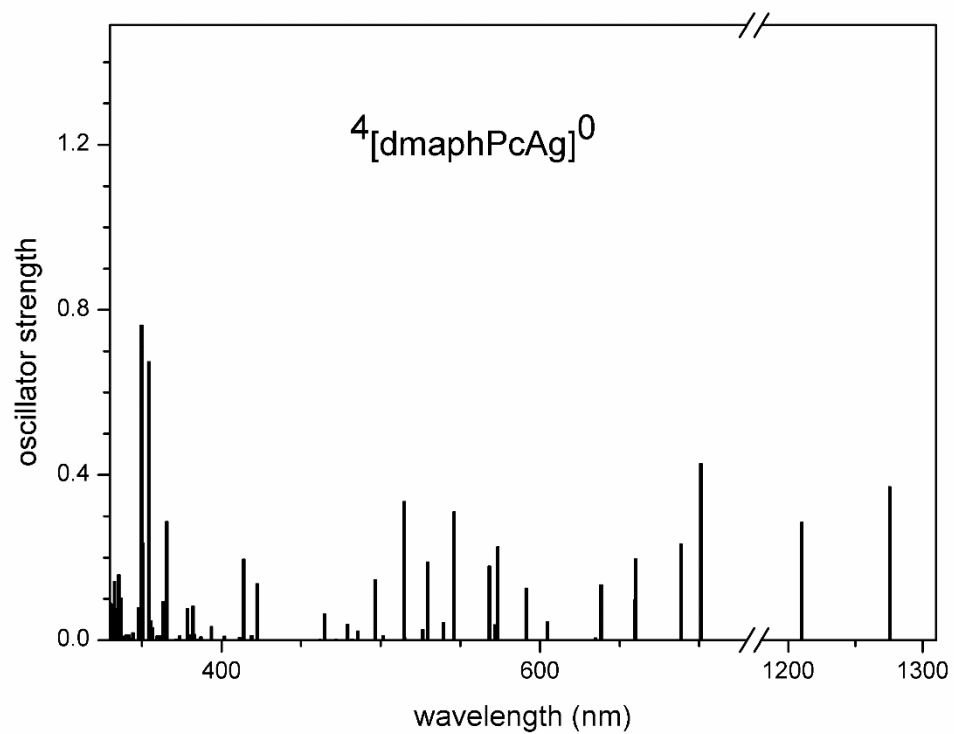


Figure S13. TD-DFT calculated electron transitions in ⁴[dmaphPcAg]⁰ in CHCl₃.

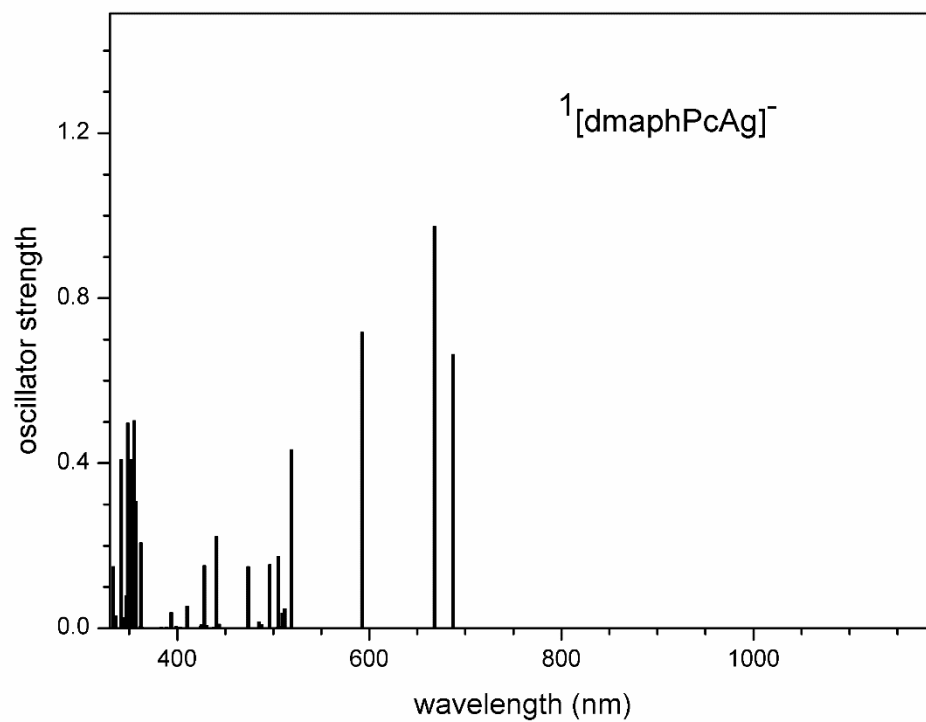


Figure S14. TD-DFT calculated electron transitions in ¹[dmaphPcAg]⁻ in CHCl₃.

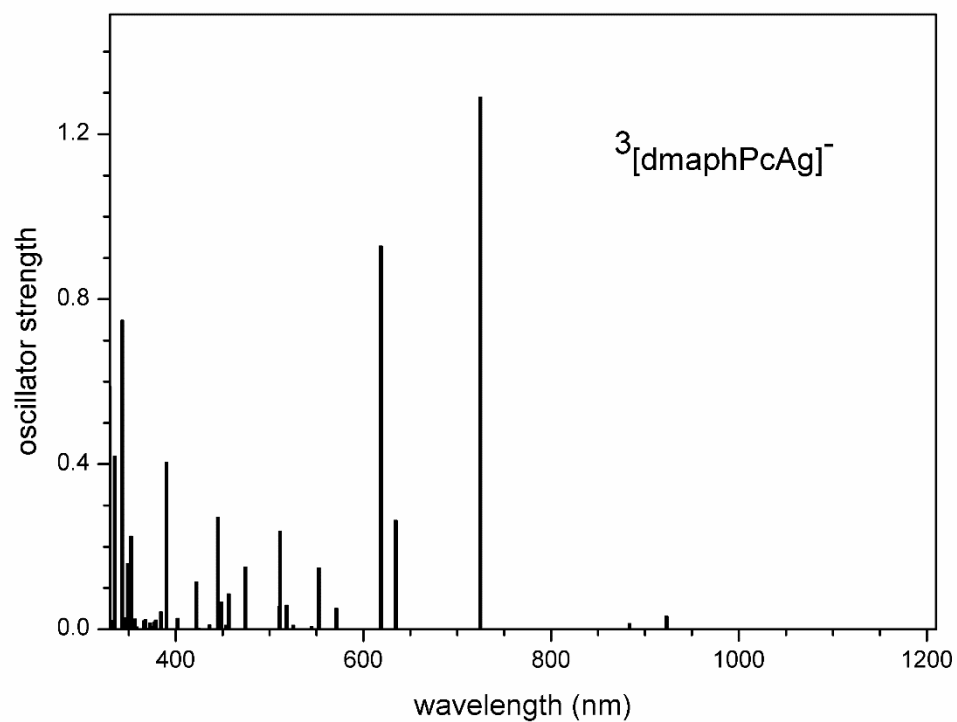


Figure S15. TD-DFT calculated electron transitions in $^3[\text{dmaphPcAg}]^-$ in CHCl_3 .

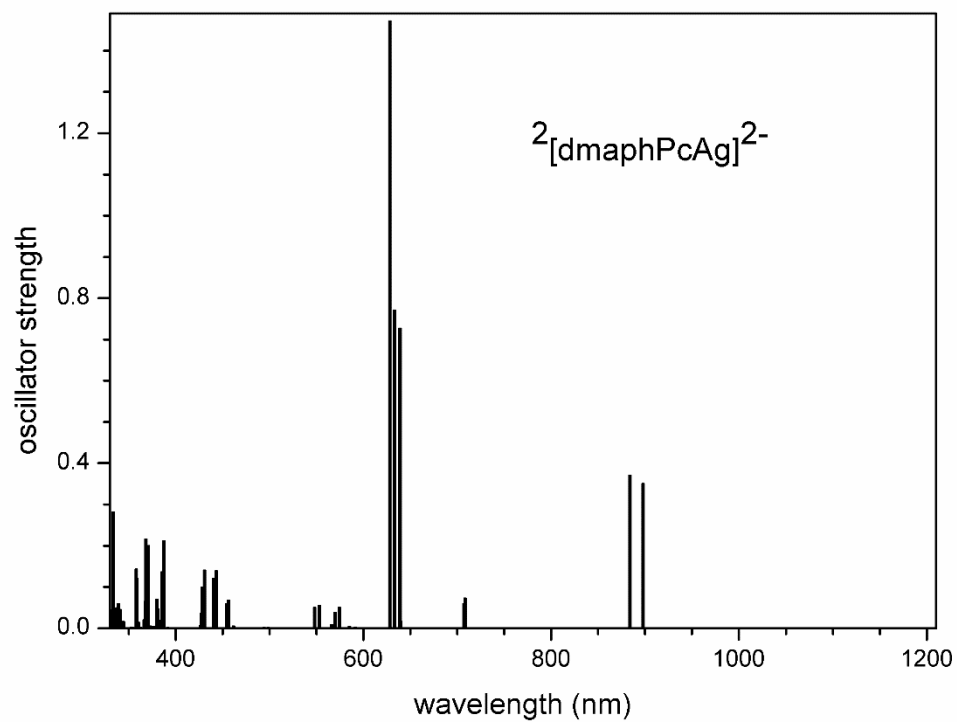


Figure S16. TD-DFT calculated electron transitions in $^2[\text{dmaphPcAg}]^{2-}$ in CHCl_3 .

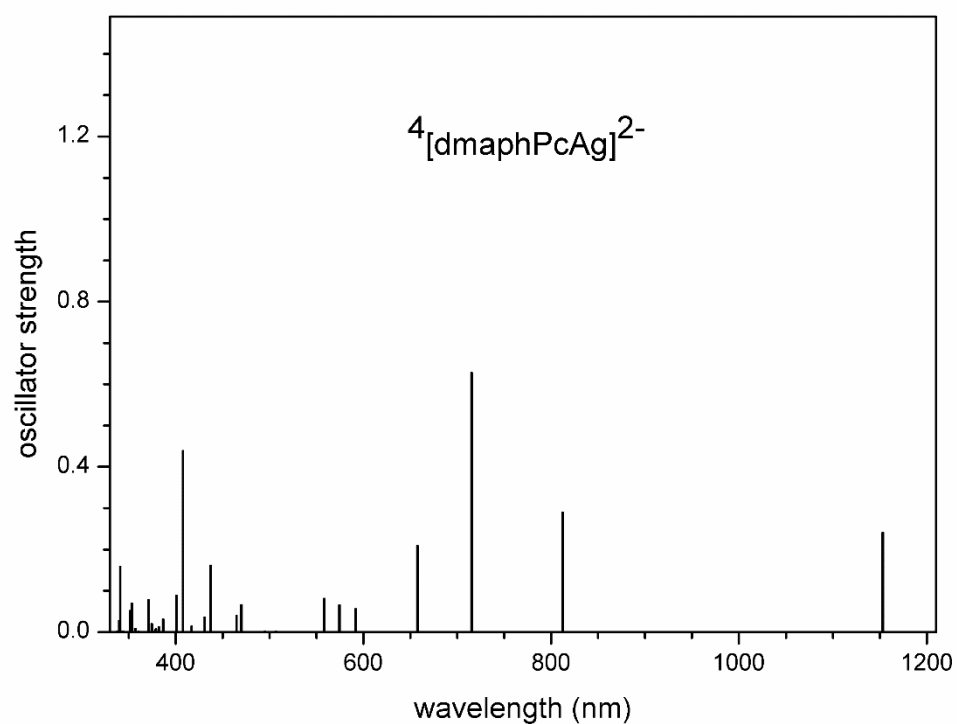


Figure S17. TD-DFT calculated electron transitions in $4[\text{dmaphPcAg}]^{2-}$ in CHCl_3 .

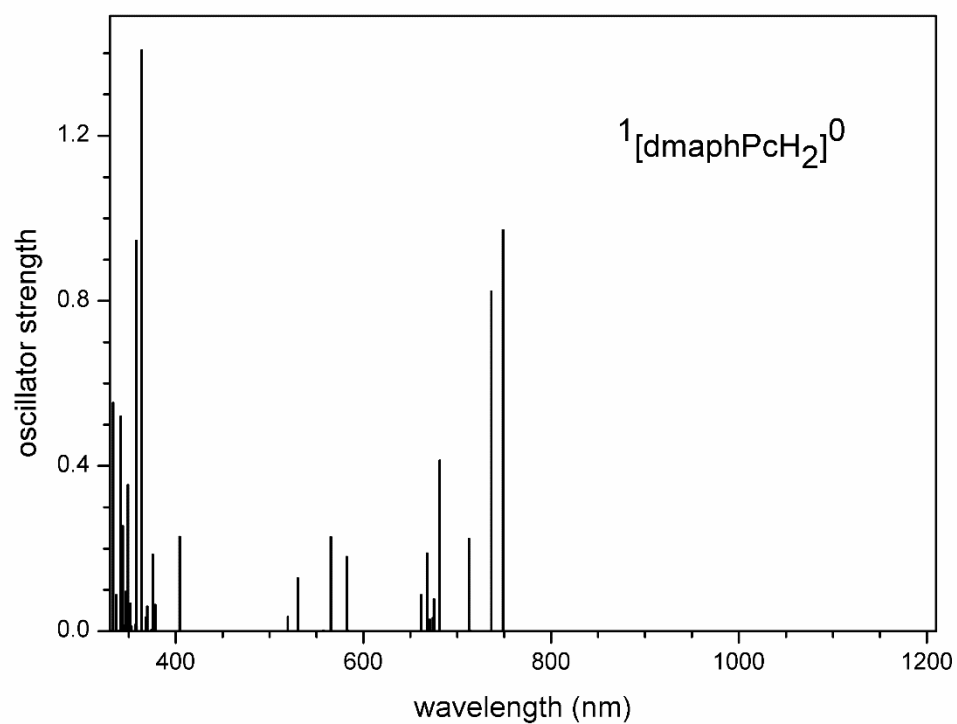


Figure S18. TD-DFT calculated electron transitions in $1[\text{dmaphPcH}_2]^0$ in CHCl_3 .

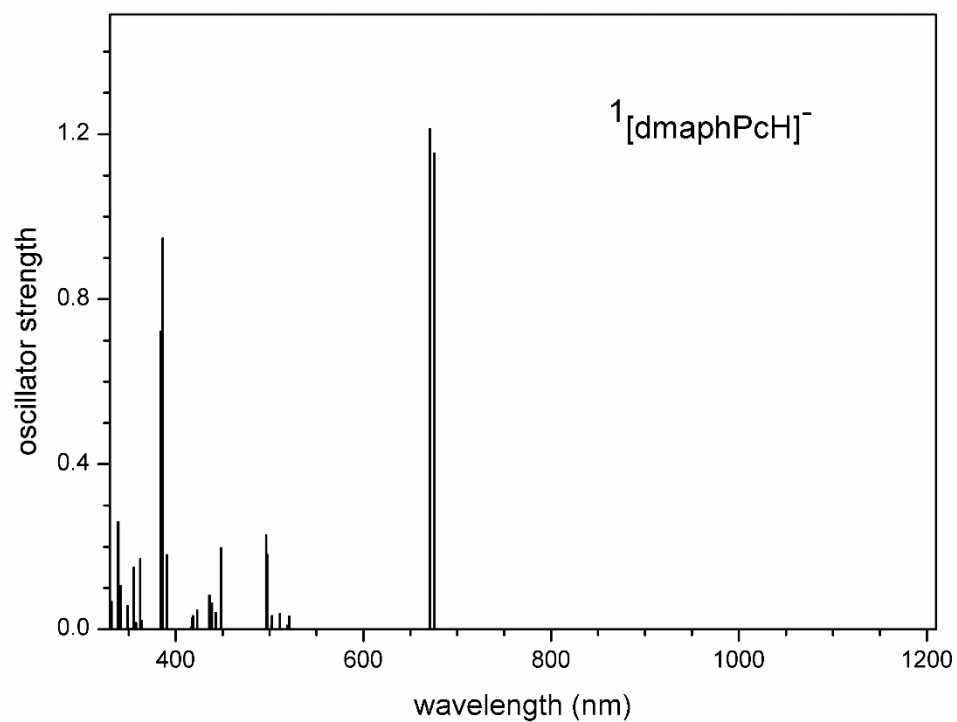


Figure S19. TD-DFT calculated electron transitions in $^1[\text{dmaphPcH}]^-$ in CHCl_3 .

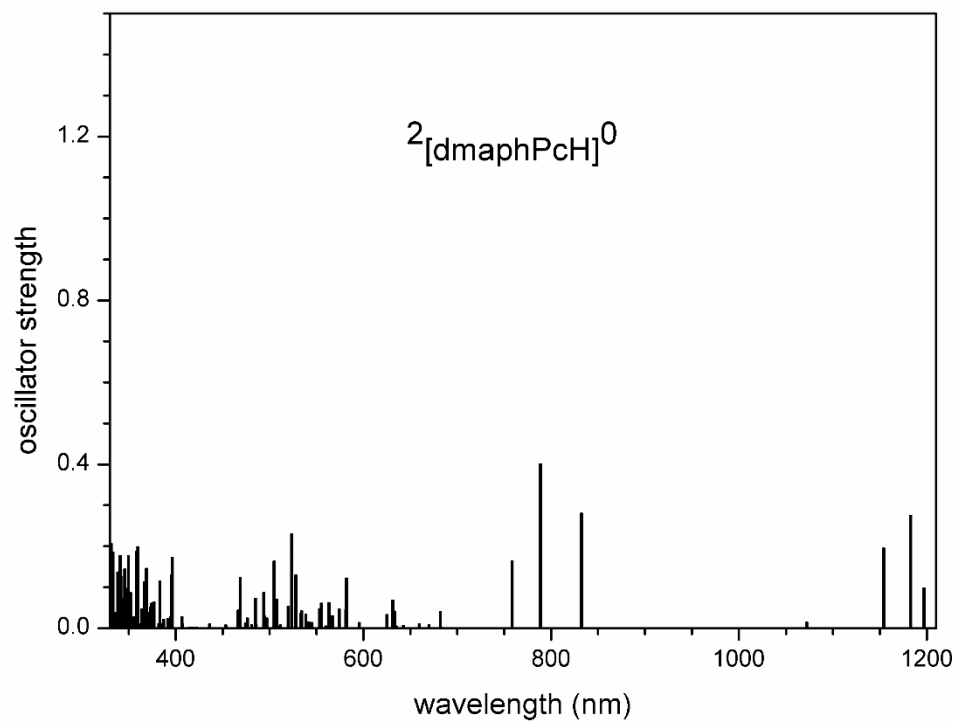


Figure S20. TD-DFT calculated electron transitions in $^2[\text{dmaphPcH}]^0$ in CHCl_3 .

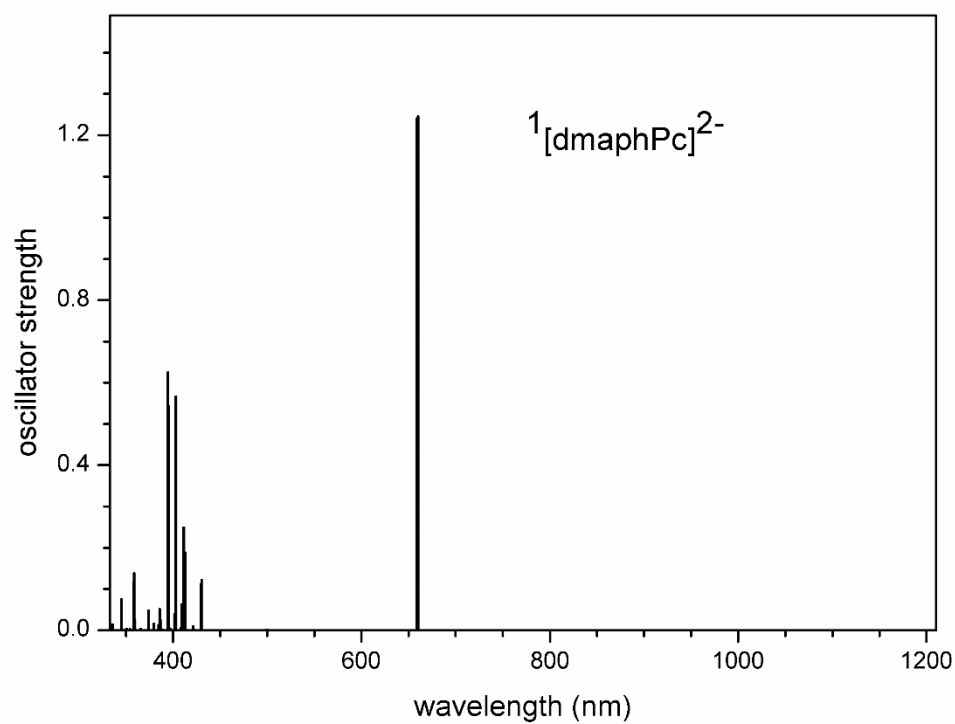


Figure S21. TD-DFT calculated electron transitions in $^1[\text{dmaphPc}]^{2-}$ in CHCl_3 .

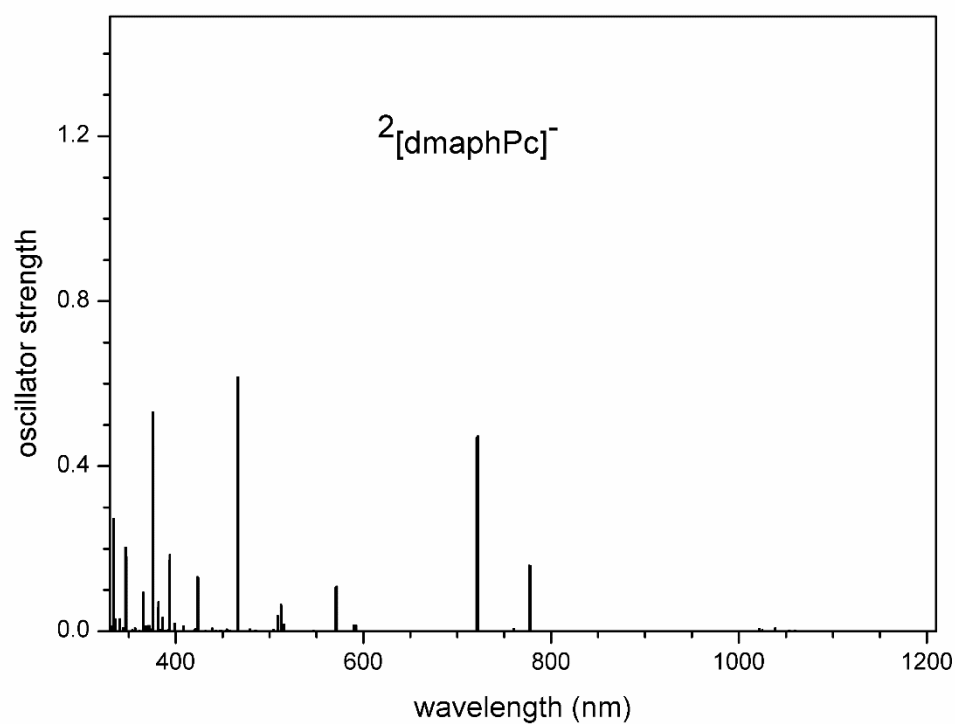


Figure S22. TD-DFT calculated electron transitions in $^2[\text{dmaphPc}]^-$ in CHCl_3 .

References

1. Breloy, L.; Alcay, Y.; Yilmaz, I.; Breza, M., Bourgon, J.; Brezová, V.; Yagci, Y., Versace, D.-L. Dimethyl amino phenyl substituted silver phthalocyanine as a UV- and visible-light absorbing photoinitiator: in situ preparation of silver/polymer nanocomposites. *Polym. Chem.* **2021**, *12*, 1273-1285.